Design of an Optimal Placement Algorithm for Large Scale Photovoltaic in Sub-Transmission Networks

Shahariar Kabir[#1], Olav Krause[#2], Ashraf Haider*[3]

[#]*School of Information Technology and Electrical Engineering, University of Queensland*
Brisbane, Australia

[1]m.kabir2@uq.edu.au

[2]o.krause@uq.edu.au

[*]*Dynamic Solution and Support Bangladesh*
Dhaka, Bangladesh

[3]ashraf.haider@dssint.com

***Abstract*— Integration of solar energy based large scale Photovoltaic (PV) unit offers significant benefits to power system. Since PV units can be installed close to load centres, improvement in reliability of network by reducing power loss and decrease in greenhouse gas emissions can be achieved. The operational characteristics and dynamics of the existing networks will be significantly influenced in near future by the continual increase in the penetration level of large scale PV. Thus, the location and sizing issues of large scale PV need to be appropriately addressed. In this paper, an algorithm is proposed to identify the optimal location and size of large scale PV in sub-transmission networks to reduce reactive power losses. The preliminary section of this paper provides literature review with specifications of IEEE 14 and 30 bus networks. Afterwards, the proposed three point loss comparison method based on exact loss formula and perturbation and observation (P&O) algorithm has been described. Then, the proposed methodology has been tested on IEEE networks. The conclusion section summarizes key findings.**

***Keywords*—contingency analysis; exact loss formulae; photovoltaic (PV); perturbation and observation (P&O); static voltage stability**

I. INTRODUCTION

In past, power systems have been designed based on unidirectional power flow concept only. But, due to the recent growing concerns about greenhouse gas emissions, fuel price hike and global warming, emphasis has been put on the integration of renewable energy based distributed generation (DG) units [1]. Among various available distributed renewable resources, integration of solar energy based Photovoltaic (PV) unit offers significant benefits to power system. PV system is capable of converting the energy obtainable in the photon of light into electricity. A PV system is superior to conventional power plants because of possessing the benefits of low maintenance cost and absence of rotating components [2]. Current technical development trends and rapid reduction in prices of PV technology indicate that the large scale application of PV will soon become one of the most commercially and economically attractive and viable sources for power generation in the world. United States of America is planning to produce 2700 MWp of electricity from Westlands Solar Park by 2015 [3]. Officials in Greece have initiated a project named Helios to construct a large scale PV site of 10,000 MWp by 2020 [4]. In Australia, it is expected that the renewable energy sources including large scale PV will produce 25% of the total electricity demand by 2020 [5]. So, it is widely anticipated that a large number of utility scale PV generators will soon be connected to the electrical transmission and sub-transmission systems in near future. Thus, the existing integration techniques and standards have to be updated as well.

By optimally placing appropriately sized large scale PV, reduction in transmission losses with improvement in terms of reliability of supply can be achieved. Since research has revealed that the optimum photovoltaic size and location greatly impact the results of integration in terms of active and reactive losses of the networks, failure to do so may result in negative consequences [6]. Thus, appropriate tools need to be developed to facilitate the sizing and location of large scale PV in sub-transmission networks.

Acharya et al. [7] presented an analytical expression to compute the optimal small scale DG size and an innovative methodology to identify the optimum location for minimizing the real power loss in primary distribution network. Afterwards, the proposed technology was verified in three distribution test systems. Based on phasor current, Wang and Nehrir [8] derived an analytical expression to optimally place distributed generation (DG) units in radial and meshed power systems to minimize power losses. Although the proposed method did not possess any convergence issue, it was only suitable for fixed size DG. Kiramani et al. [9] applied heuristic search algorithm for the optimal placement of small scale PV system to reduce the real power loss in radial distribution network. Carpinelli et al. [10] utilized genetic algorithm based technique to determine the appropriate size and location of small scale DG units such as PV. Though, genetic techniques were identified as an appropriate tool for solving multi-objective based problems such as DG allocation providing

near optimal results, amount of computations required to perform the task was regarded as the major drawback. Willis [11] proposed a "2/3 rule" to optimally place DG on a radial feeder with homogeneously distributed loads. It was suggested to locate small scale DG units including PV of approximately 2/3 of the capacity of the incoming generation at approximately 2/3 of the length of transmission line. Though the proposed method was uncomplicated, this could not be utilized to a feeder with different load distribution or to networked systems. Krueasuk and Ongsakul [12] utilized particle swarm optimization (PSO) method to optimally place small scale DG units in a primary distribution network to reduce the total real power loss. By means of the proposed algorithm, improvement in voltage profiles and reduction in branch currents were achieved. Ameli et al. [13] utilized fuzzy logic algorithm to optimally place distributed generation units to improve the voltage profiles and reduce losses in distribution networks. This analysis concluded that the location, type and sizing aspects greatly influenced the performance of DG in distribution feeders.

Although, a number of studies have been performed in the past in the field of loss reduction with the integration of small scale DG including PV, in these studies, the impact of large scale PV units has not been adequately assessed. Thus, the purpose of this paper is to present an algorithm based on exact loss formula and perturbation and observation (P&O) method to determine the appropriate size and location of unity power factor operated large scale PV to reduce reactive power losses in sub-transmission networks. Remaining of the paper is organized as follows: Section II presents details of IEEE 14 and 30 bus networks used in the presented studies. Section III describes the modelling of PV system. Section IV illustrates the technology known as three point loss comparison method to determine the optimal size and location of PV. Afterwards, the proposed technology has been verified in section V with respect to IEEE reference test networks. The conclusion section summarizes key findings.

II. NETWORK CONFIGURATION

In this study, IEEE 30 and 14 bus sub-transmission networks have been utilized as depicted in Figures 1-2 [14]. These two networks have been selected as they are widely used in loss reduction studies [14].

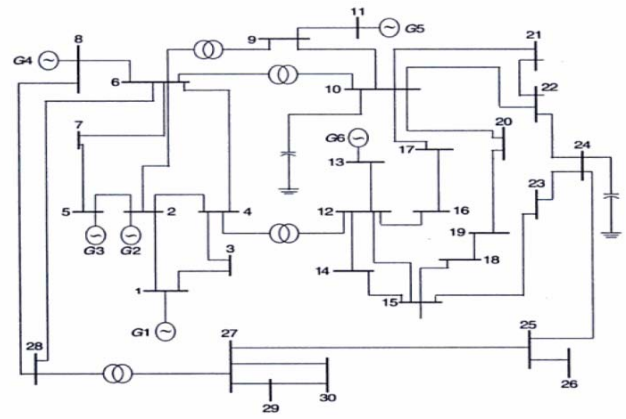

Figure 1. Schematic diagram of implemented IEEE 30 bus system.

The considered 30 bus sub-transmission network consists of six synchronous generators, thirty buses, forty-one branches and four transformers. The network possesses twenty one load points with a loading level of 283.4 MW and 100.95 MVAR. Shunt impedances are located at bus 10 and 24. Network data of the implemented system is available from [14].

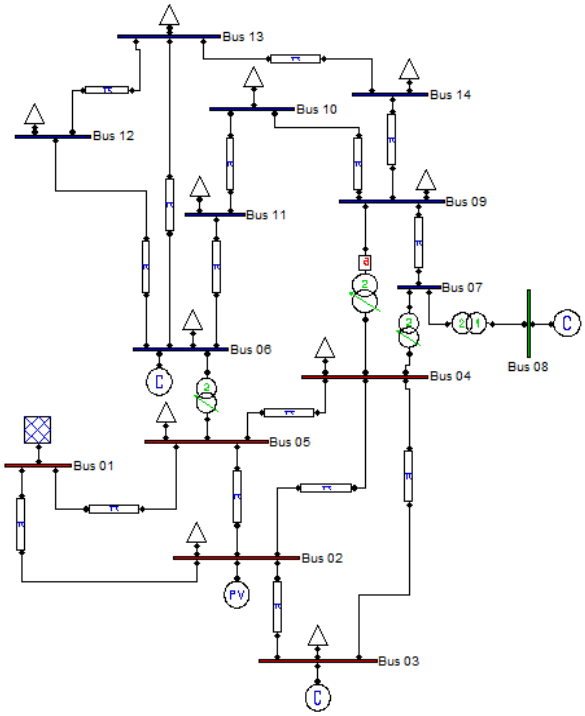

Figure 2. Schematic diagram of implemented IEEE 14 bus system.

The considered 14 bus sub-transmission network consists of five synchronous machines, twenty branches, four transformers and eleven constant power (PQ) loads. The loading level has been selected as 362.6 MW and 113.96 MVAR. Three synchronous machines located at bus 3, 6 and 8 are used for reactive power support only. The remaining two located at bus 1 and 2 are used as synchronous generators. Network data of the implemented system is available in [14].

III. MODELLING OF GRID CONNECTED PV SYSTEM

A PV cell consists of an ideal current source, diode, series resistance and parallel resistance that have been characterized by following equations in this paper [15]:

$$I = I_{sc} - I_o\left(e^{\frac{qV_d}{nKT}} - 1\right) - \frac{V_d}{R_p} \quad (1)$$

$$V_d = V + IR_s \quad (2)$$

where, V, I = output voltage and current (V, A), n = emission coefficient factor, I_{sc} = short circuit current (A), I_o = diode reverse saturation current (A), q = electron charge (1.602×10^{-19} C), V_d = diode voltage (V), K = boltzmann's constant ($1.381 \times 10^{-23} JK^{-1}$) and T = cell temperature (K).

In this paper, a single-generator equivalent double stage configured unity power factor operated large scale PV unit

with DC-DC boost converter and DC-AC self-commutated inverter has been implemented as depicted in Fig. 3.

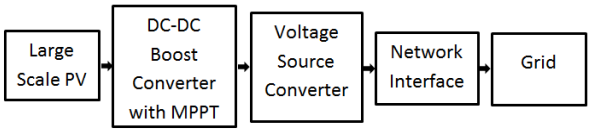

Figure 3. Structural diagram of applied grid connected large scale PV.

Incremental conductance algorithm has been used to perform maximum power tracking (MPPT). Voltage source converter (VSC) configuration has been implemented to convert the dc voltage of PV into AC. Proportional-Integral (PI) algorithm based decoupled current controllers have been implemented to independently control the injections of active (P_{ac}) and reactive (Q_{ac}) powers that have been represented by following equations [16] :

$$P_{ac} = \frac{0.6128 m V_s V_A \sin\delta}{X_t} \quad (3)$$

$$Q_{ac} = 0 \quad (4)$$

where, V_s = grid voltage (V), V_A = PV terminal voltage (V), X_t = impedance between inverter and grid terminals (Ω), m = modulation parameter and δ = phase angle (rad).

IV. Design of an Optimal Placement Algorithm

To define the penetration level of large scale PV, the formula stated below has been used in this paper [17-18]:

$$\text{Penetration Level } (\%) = \frac{\sum P_{LPV}}{\sum P_{Load}} \text{ x } 100 \quad (5)$$

where, P_{LPV} = installed generation capacity of large scale PV (W) and P_{Load} = maximum real power load demand that can be met by generators (W). It is presumed in this paper that the PV units operate at 100% of their capacity.

Simulation results have revealed that the reactive power loss of sub-transmission network with respect to the size of integrated large scale PV is a parabolic function. Thus, to formulate the proposed three point loss comparison algorithm based on exact loss formula and perturbation and observation (P&O) method to obtain the optimum size and location of unity power factor operated large scale PV to reduce reactive power loss, the following three steps have been followed:

A. Determination of the Approximate Size of PV via Exact Loss Formula

According to exact loss formula [19]:

$$Q_{loss} = \sum_{i=1}^{N} \sum_{j=1}^{N} [\alpha_{ij}(P_i P_j + Q_i Q_j) + \beta_{ij}(Q_i P_j - P_i Q_j) \quad (6)$$

where:

$$\alpha_{ij} = \frac{x_{ij}}{V_i V_j} \cos(\delta_i - \delta_j) \text{ and } \beta_{ij} = \frac{x_{ij}}{V_i V_j} \sin(\delta_i - \delta_j) \quad (7)$$

Here, x_{ij} = reactance of a line between bus i and j (Ω), P_i and P_j = active power injections at bus i and j respectively (W), Q_i and Q_j = reactive power injections at bus i and j respectively (VAR), V_i and δ_i = ith bus voltage magnitude and angle respectively (V, rad), V_j and δ_j = voltage magnitude and angle respectively for bus j (V, rad). Thus, after the integration of unity power factor operated large scale PV, the injected bus real power is obtained by following [7]:

$$P_i = P_{PVi} - P_{Loadi} \quad (8)$$

where, P_{PVi} = real power injection from PV unit at bus i (W) and P_{Loadi} = real component of load at bus i (W). So, reactive power loss formula is transformed into following:

$$Q_{LossPV} = \sum_{i=1}^{N} \sum_{j=1}^{N} [\alpha_{ij}((P_{PVi} - P_{Loadi}) P_j + Q_i Q_j) + \beta_{ij} (Q_i P_j - (P_{PVi} - P_{Loadi}) Q_j)] \quad (9)$$

At lowest reactive power loss point:

$$\frac{dQ_{LossPV}}{dP_{PVi}} = 0 \quad (10)$$

Thus, the approximate size of large scale PV:

$$P_{PVi} = P_{Loadi} + \frac{1}{\alpha_{ii}} [\beta_{ii} Q_i - \sum_{j=1,\ j \neq i}^{N} (\alpha_{ij} P_j - \beta_{ij} Q_j)] \quad (11)$$

After the installation of large scale PV unit in the network, the values of loss coefficients change due to state variables such as voltage and angle. Thus, the approximate size of large scale PV in (11) is obtained from the base case co-efficient values as per (7).

B. Determination of the Exact Size of PV via Perturbation and Observation Algorithm

With respect to the calculated approximate PV sizes from step A, to define the exact sizes with lowest losses, Table I have been formulated.

TABLE I. Table of Perturbation and Observation Rule

Perturbation in PV size	Change in Differences in Reactive Power Losses Between Point i and (i-1)	Next Perturbation in PV size
Positive	Positive	Negative
Positive	Negative	Positive
Negative	Negative	Negative
Negative	Positive	Positive

According to the perturbation and observation theory, larger perturbation size helps to achieve faster calculation of desired point though the accurateness is negatively impacted. On the other hand, smaller perturbation step helps to attain higher accuracy at the expense of calculation speed [20]. To improve both properties, a variable perturbation size concept to determine the exact PV size has been introduced in this paper. In this technique, the slope of the reactive loss curve is used as a measure of closeness to the designed solution. To strike a compromise between accuracy and precision, perturbation step size is gradually reduced as the steepness of the curve lowers.

C. Confirmation of Results

The results achieved in step 2 are confirmed via three point loss comparison method as depicted in Fig. 4.

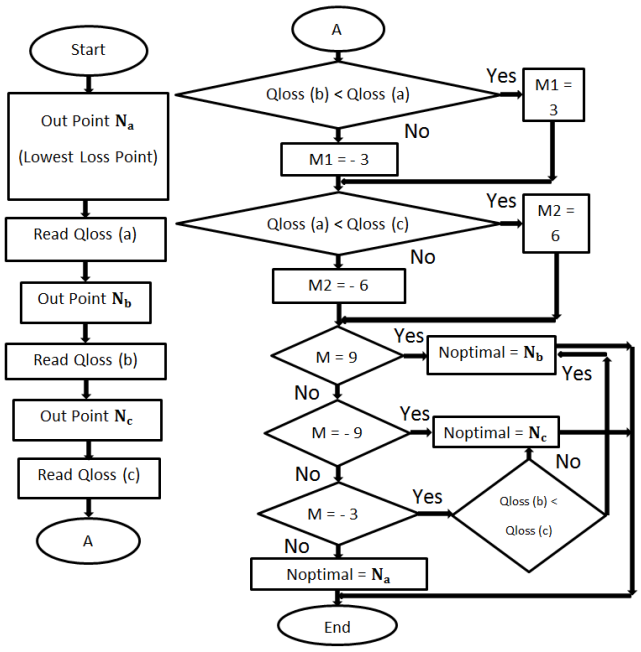

Figure 4. Flowchart of proposed three point loss comparison method.

Initially, the point (N_a) with the lowest reactive power loss as calculated by (10) is selected with the preceding (N_b) and succeeding (N_c) ones. Afterwards, based upon the comparison results and the formula (M = M1+M2), exact size of large scale PV at each bus obtained via step 2 is verified to determine the optimal value. Therefore, according to the proposed method, the allocation procedure of large scale PV has been designed to resolve the sizing issue first at each bus followed by the optimal location issue. The overall computational procedure has been depicted below:

(1) Run the base case power flow without PV.

(2) Find the optimum size of large scale PV for each bus using the proposed three point loss comparison method.

(3) Calculate the exact reactive power loss for each bus with PV by means of (9).

(4) Identify the bus at which the reactive power loss is minimum to be regarded as the best candidate for allocation.

(5) Run the concluding power flow with PV to verify the results.

In this paper, the following constraints have been specified:

- Bus voltage with PV is within upper and lower limits [1].
- The new reactive power loss with PV is less than the base case.
- Maximum penetration level of large scale PV is 25% as per (5) [5].

V. Discussion of Results

Without PV, for IEEE 14 bus network, the reactive power loss has been noted as 92.16 MVAR. The obtained results for IEEE 14 bus system (excluding slack bus) in terms of reactive power losses have been depicted in Fig. 5.

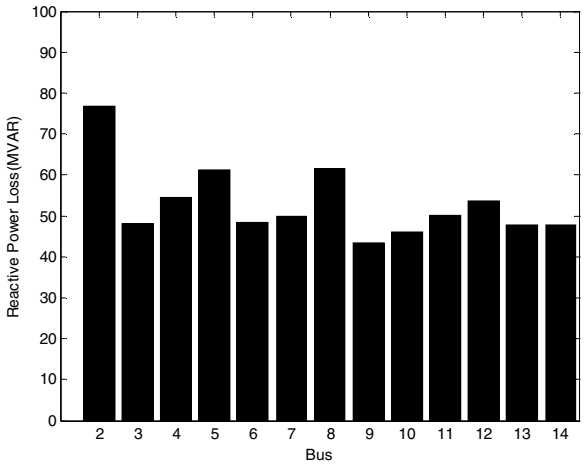

Figure 5. Reactive power losses of IEEE 14 bus system with PV.

Slack bus has been excluded from analysis as the integration of PV at slack bus does not produce any significant outcome in terms of reactive power loss reduction. Thus, it can be concluded from Fig. 5 that the integration of large scale PV provides positive impact in terms of reactive power loss reduction in IEEE 14 bus network. Power losses vary between 43.54 - 76.78 MVAR after integrating PV with a size range of 84.58 - 90.62 MW and non-generator bus 9 has been identified as the best location.

To analyse the impact of placing large scale PV at the bus with lowest reactive power loss on static voltage stability, the following analyses have been performed: Saddle node bifurcation is recognized as one of the most significant static factors for voltage stability issues in power system. According to this bifurcation theorem [21]:

$$g(y,\lambda) = 0 \quad (12)$$

$$\nabla_y g(y,\lambda)v = 0 \quad (13)$$

$$|v|=1 \quad (14)$$

or

$$g(y,\lambda) = 0 \quad (15)$$

$$\nabla_y g(y,\lambda)^T w = 0 \quad (16)$$

$$|w|=1 \quad (17)$$

where, w and v are the left and right eigenvectors respectively. After the integration of 90.62 MW PV at bus 9, the maximum loading margin of the network increases by 10.54%. During contingency analysis, the figure has been identified as 10.82% for the loss of transmission line from bus 5-4, 11.82% for the loss of synchronous generator at bus 2 and 11.53% for the loss of reactive power compensation unit at bus 8.

Synchronous generator reactive power limit induced bifurcation has been incorporated in this paper as per following [22]:

$$Q_i^{gmin} \leq Q_i^{g} \leq Q_i^{gmax} \ (i = 1, 2, \dots, n) \quad (18)$$

After the integration of PV at bus 9, the maximum loading margin with respect to the synchronous generator reactive power limit induced bifurcation has been increased by 12.48%. The figure has been noted as 15.44% for the loss of transmission line from bus 5-4, 11.38% for the loss of synchronous generator at bus 2 and 12.30% for the loss of reactive power compensation unit at bus 8.

During limit induced bifurcation, the lack of steady state solution is due to the system controls reaching generator control or transmission network power flow limits [22]. With standard network, the maximum loading margin during transmission network MVA flow constrained analysis has been calculated as per following formula [22]:

$$S_{ij} \leq S_{ijmax} \quad (19)$$

After the integration of PV at bus 9, the maximum loading margin with respect to the transmission network MVA flow constrained bifurcation has been increased by 10.54%. The figure has been identified as 10.82% for the loss of transmission line from bus 5-4, 11.82% for the loss of generator at bus 2 and 11.53% for the loss of reactive power compensation unit at bus 8. Thus, it can be also observed that the saddle node bifurcation occurs before transmission network MVA flow constrained bifurcation in IEEE 14 bus system.

The singular values of Jacobian matrix attained via singular value decomposition (SVD) analysis are widely utilized to evaluate voltage stability [23]. The power flow equation depicted in (20) has been considered in this paper [23].

$$\begin{bmatrix} \Delta P \\ \Delta Q \end{bmatrix} = \begin{bmatrix} J_{11} & J_{12} \\ J_{21} & J_{22} \end{bmatrix} \begin{bmatrix} \Delta\theta \\ \Delta V \end{bmatrix} \quad (20)$$

where, P = active power (W), Q = reactive power (VAR), θ = node angle (rad), V = node voltage (V) and J = jacobian matrix of standard power flow. According to the theorem [24]:

$$J = L \Lambda R^{T} \quad (21)$$

$$= \sum L_j \Lambda_j R_j^{T} \ (j = 1, 2, \dots, n) \quad (22)$$

where, Λ_j = singular values, R_j and L_j = right and left singular vectors respectively. Thus, for a non-singular Jacobian matrix, the minimum singular value describes the closeness to voltage collapse. With PV at bus 9, the relative stability of the network improves by 5.95%. The figure has been calculated as 6.71% for the loss of transmission line from bus 5-4, 9.05% for the loss of synchronous generator at bus 2 and 7.86% for the loss of reactive power compensation unit at bus 8.

Modal analysis defines power system's proximity to voltage collapse while detecting the causes of instability. According to the theorem, after letting ΔP = 0 in (20), the characteristic equation is obtained as per (23) [25].

$$\Delta Q = [\, J_{22} - J_{21} J_{11}^{-1} J_{12}] \, \Delta V = J_R \, \Delta V \quad (23)$$

Thus, the voltage stability features of the designed network can be investigated by computing eigenvalues of J_R (reduced Jacobian matrix) as the eigenvalues classify operational modes through which instability can occur in the network. Value of the minimum eigenvalue characterizes a relative measure of proximity to voltage collapse. With large scale PV at bus 9, the minimum eigenvalue of the network improves by 0.6%. The figure has been found as 0.83% for the loss of transmission line from bus 5-4, 0.72% for the loss of generator at bus 2 and 0.9% for the loss of reactive power compensation unit at bus 8. Thus, it can be concluded that the integration of appropriately sized large scale PV at the bus with lowest reactive power loss positively influences the static voltage stability of IEEE 14 bus network. However, it should be noted that if the key objective is to achieve the best results in terms of network's static voltage stability, the calculated values may not be the optimal choices in this regard.

For IEEE 30 bus system, the following loss characteristics figure (excluding slack bus) has been noted:

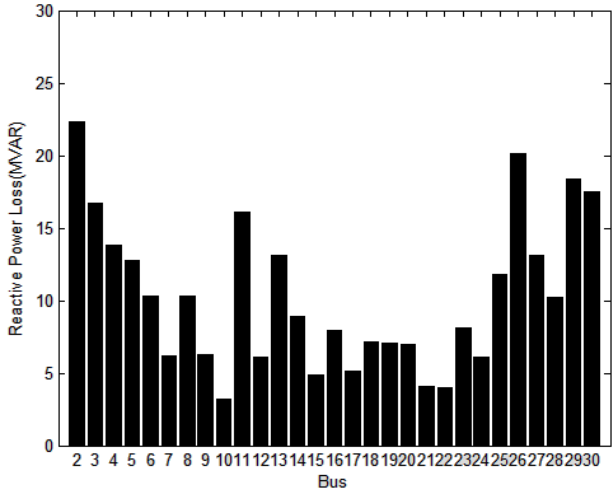

Figure 6. Reactive power losses of IEEE 30 bus system with PV.

Thus, the usefulness of large scale PV in terms of reactive power loss reduction has been proved from Fig. 6 with respect to the base case loss of 32.68 MVAR. Bus 10 which is a non-generator bus has been identified as the best location to reduce reactive power loss. The power losses vary between 3.22-22.34 MVAR with a PV size range of 41.56 - 70.85 MW.

To analyse the impact of inserting 70.85 MW sized PV at bus 10 on static voltage stability of IEEE 30 bus system, the following analyses have been performed: With respect to the standard maximum loading margin as per (12 -17), with PV, the maximum loading margin improves by 3.6%. The figure has been calculated as 3.63% for the loss of transmission line from bus 12-14, 4.5% for the loss of reactive power compensation unit at bus 11 and 6.21% for the loss of generator at bus 2.

With respect to the synchronous generator reactive power limit induced bifurcation as per (18), after the integration of PV at bus 10, the maximum loading margin has improved by 11.31%. The figure has been noted as 11.37% for the loss of transmission line from 12-14, 11.85% for the loss of reactive

power compensation unit at bus 11 and 11.5% for the loss of synchronous generator at bus 2.

With respect to transmission network MVA flow constrained bifurcation as per (19), after integrating PV at bus 10, the maximum loading margin improves by 3.6%. The figure has been calculated as 3.63% for the loss of transmission line at bus 12-14, 4.5% for the loss of reactive power compensation unit at bus 11 and 6.21% for the loss of synchronous generator at bus 2. It has been also noted that the saddle node bifurcation occurs before transmission network MVA flow constrained bifurcation in IEEE 30 bus network like previously described 14 bus system.

After performing singular value decomposition analysis as per (21-22), it has been noted for standard case that the inclusion of 70.85 MW PV at bus 10 improves the relative stability of the network by 3.34%. During contingency analysis, the following figures have been noted: 3.39% for the loss of transmission line from bus 12-14, 4.01% for the loss of reactive power compensation unit at 11 and 4.43% for the loss of generator located at bus 2.

After performing modal analysis as per (23), with large scale PV at bus 10, the minimum eigenvalue of the network improves by 0.45%. The figure has been calculated as 0.50%, 0.98% and 0.58% for the loss of transmission line (bus 12-14), reactive power compensation unit (bus 11) and synchronous generator (bus 2) respectively.

VI. CONCLUSION

This research paper presents an accurate and fast algorithm to identify the optimum location and size of large scale PV units in sub-transmission networks to reduce reactive power losses. It can be concluded that the integration of large scale unity power factor operated PV unit provides positive outcome in terms of reactive power loss reduction. Location and size of PV are crucial factors in this application. It can be also observed that the integration of appropriately sized large scale PV at the bus with the minimum reactive power loss positively influences the static voltage stability of sub-transmission networks.

ACKNOWLEDGMENT

The authors would sincerely like to acknowledge Professor Simon Bartlett, Professor Tek Tjing Lie and Dr. Ramesh Bansal for their help and contributions in developing this research paper.

REFERENCES

[1] G. Mills, S. Franklin, R. Passey, M. Watt, A. Bruce, and W. Johnson. (2011,Nov.). Modeling of Large-Scale PV Systems in Australia. Australian PV Ass., Australia. [Online]. Available: http://control.visionscape.com.au/SiteFiles/australiansolarinstitutecomau/ModellingofLargeScalePVSystemsinAustralia.pdf

[2] M. A. Eltawil and Z. Zhao, "Grid-connected photovoltaic power systems: Technical and potential problems − A review," *Renewable and Sustainable Energy Reviews*, vol. 14, pp. 112-129, 2010.

[3] J. H. R. Enslin, "Dynamic reactive power and energy storage for integrating intermittent renewable energy," in *Proc. IEEE Power and Energy Society General Meeting,* 2010*,* pp. 1– 4.

[4] (2010) The Wikipedia website. [Online]. Available: http://en.wikipedia.org/wiki/Solar_power_in_Greece

[5] (2009) The Australian Government website. [Online]. Available: http://www.climatechange.gov.au/government/initiatives/renewable-target.aspx

[6] K. S. Rao and M. N. Rao, "Optimal Placement of Multiple Distributed Generator by Hs Algorithm," *Int. J. Eng. Research and Appl.*, vol. 2, pp. 1290-1294, 2012.

[7] N. Acharya, P. Mahat, and N. Mithulanthan, "An analytical approach for DG allocation in primary distribution network," *Int. J. Elect. Power and Energy Syst.,* vol. 28, pp. 669-678, 2006.

[8] C. Wang and M. H. Nehrir, "Analytical approaches for optimal placement of distributed generation sources in power systems," *IEEE Trans. Power Syst.,* vol. 19, pp. 2068−2076, 2004.

[9] S. Kirmani, M. Jamil, and M. Rizwan, "Optimal Placement of SPV based DG System for Loss Reduction in Radial Distribution Network Using Heuristic Search Strategies," in *Proc. IEEE 2nd International Power and Energy Conf.,* 2008*,* pp. 1691-1695.

[10] G. Carpinelli, G. Celli, and A. Russo, "Distributed generation siting and sizing under uncertainty," *in Proc. IEEE Porto power tech.,* 2001*,* pp. 1-7.

[11] H. L. Willis, "Analytical methods and rules of thumb for modeling DG-distribution interaction," in *Proc. IEEE Power Eng. Society Summer Meeting,* 2000*,* pp. 1643 – 1644.

[12] W. Krueasuk and W. Ongsakul, "Optimal Placement of Distributed Generation Using Particle Swarm Optimization," in *Proc. Australian Universities Power Eng. Conf.,* 2006*,* pp. 1-6.

[13] M. Ameli, V. Shokri, and S. Shokri, "Using fuzzy logic amp; full search for distributed generation allocation to reduce losses and improve voltage profile," in *Proc. Int. Conf. on Computer Inf. Syst. and Industrial Management Appl.,* 2010*,* pp. 626–630.

[14] F. Milano, *Power system modeling and scripting*, *vol. 1*. London: Springer, 2010.

[15] Y. J. Wang and P. C. Hsu, "Analytical modeling of partial shading and different orientation of photovoltaic modules," *IET Renewable Power Gen.*, vol. 4, pp. 272-282, 2010.

[16] X. Xiaoyan, H. Yuehui, H. Guoqing, Z. Haixiang, and W. Weisheng, "Modeling of large grid-integrated PV station and analysis its impact on grid voltage," in *Proc. Int. Conf. on Sustainable Power Generation and Supply,* 2009*,* pp. 1-6.

[17] T. Aziz, S. Dahal, N. Mithulananthan, and T. K. Saha, "Impact of Widespread Penetrations of Renewable Generation on Distribution System Stability," in *Proc. 6th Int. Conf. on Elect. and Computer Eng.,* 2010*,* pp. 338 – 341.

[18] R. Shah, N. Mithulananthan, and R. C. Bansal, "Damping performance analysis of battery energy storage, ultracapacitor and shunt capacitor with large-scale PV plants," *Appl. Energy Spec. Issue Smart Grid*, vol. 96, pp. 235–244, 2012.

[19] P. Kundur, *Power System Stability and Control*, vol. 2. New York: McGraw-Hill, 1994.

[20] T. Esram and P. L. Chapman, "Comparison of Photovoltaic Array Maximum Power Point Tracking Techniques," *IEEE Trans. Energy Conv.,* vol. 22, pp. 439-449, 2007.

[21] D. P. Kothari and J. S. Dhillon, *Power System Optimization*, vol. 3. New Delhi: Prentice Hall of India Pvt. Ltd., 2006.

[22] V. Ajjarapu and B. Lee, "Bibliography on voltage stability," *IEEE Trans. Power Syst.,* vol.13, pp. 115−125, 1998.

[23] M. Dehghani, B. Shayanfard, and A. R. Khayatian, "PMU Ranking Based on Singular Value Decomposition of Dynamic Stability Matrix," *IEEE Trans. Power Syst.,* vol. PP, pp. 1-8, 2013.

[24] K. Ellithy, M. Shaheen, M. Al-Athba, A. Al-Subaie, S. Al-Mohannadi, S. Al-Okkah, and S. Abu-Eidah, "Voltage stability evaluation of real power transmission system using singular value decomposition technique," in *Proc. IEEE 2nd Int. Power and Energy Conf.,* 2008*,* pp. 1691-1695.

[25] C. Sharma and M. G. Ganness, "Determination of Power System Voltage Stability Using Modal Analysis," in *Proc. Int. Conf. on Power Eng*., Energy and Elect. Drives, 2007, pp. 381 – 387.